Published online June 27, 2017

Methods of Soil Analysis

Field Measurements of Soil Cracks

Ryan D. Stewart* and Majdi R. Abou Najm

Shrink–swell soils, often classified as Vertisols or vertic intergrades, are found worldwide and are a leading cause of damage to infrastructure such as buildings, roads, and pipelines. Crack networks act as dominant environmental controls on the movement of water, contaminants, and gases. Numerous methods have been proposed to quantify the size (e.g., width, depth, volume) and connectivity of individual cracks and of larger crack networks. To measure and quantify the size and variability of cracks, we focus on two nondestructive methods, called here the *tape and rod* and *displacement* approaches, and one destructive method, called here the *cast and excavate* protocol. The nondestructive methods are relatively inexpensive and can allow repeated measurements, which makes them conducive to use in larger environmental studies such as observing hydrological partitioning between infiltration and surface runoff. However, the nondestructive methods are often biased toward larger cracks (due to physical limitations on the crack sizes that can be measured), require assumptions of crack geometry to determine crack volumes, and typically do not provide information on subsurface connections between cracks. The destructive cast and excavate method is better suited to sample a range of crack sizes and can be used to better understand subsurface connectivity, although it oftentimes can only be used once (precluding repeated measurements) and is labor intensive. A combination of measurements may therefore be required to best understand crack dynamics in both time and space. Altogether, the methods surveyed here enable accurate measurement and quantification of soil crack characteristics.

Shrink–swell soils, often classified as Vertisols or vertic intergrades, are found worldwide. Within the United States, surface soils with linear extensibility ratings of moderate (3–6%), high (6–9%) and very high (>9%) occupy approximately 40% of the land area (Fig. 1). Such soils are a leading cause of damage to infrastructure, including roadways (Stavridakis, 2006), buildings (Jones and Jefferson, 2012), and buried pipelines (Hudak et al., 1998). Previous estimates have held that expansive soils have damaged one in four homes in the United States (Krohn and Slosson, 1980), resulting in billions of dollars of related costs. As urban areas continue to expand, problems caused by shrink–swell soils will probably increase, making proper understanding and management of expansive clay soils a high priority.

Vertic soils are generally characterized by high clay contents (>30%), often with a large proportion of swelling 2:1 clays (e.g., montmorillonite). Due to their mineral structure, these 2:1 clay particles experience substantial volume changes as they wet and dry. Because of this volume change, shrinkage cracks of varying size and complexity can form as the soil profile dries. When open, these cracks can act as preferential flow paths for infiltrating water (Wopereis et al., 1994; Favre et al., 1997; Stewart et al., 2015), as well as conduits by which water vapor and other gases are readily exchanged with the atmosphere (Weisbrod et al., 2009). Their contribution to flow can vary considerably even within the same soil (Sanders et al., 2012), depending on a wide range of factors, including pore structure and connectivity, surface conditions, vegetation, and initial moisture condition. Quantifying the size and connectivity of cracks is necessary to predict the movement of water, solutes, and gases into and through the landscape. This need has led to the development of a multitude of methods to measure and analyze soil cracking.

REVIEW OF EXISTING PROCEDURES

Accurate quantification of soil crack volume and connectivity is a challenging undertaking, for which a number of different methods have been proposed. In general, these techniques may be divided into two broad categories: nondestructive and destructive. Nondestructive methods work best in conjunction with other complementary measurements (e.g., infiltration rates, soil water content, gas exchange rates) or when repeated measurements are required. However, nondestructive measures often have lower accuracy and provide less information than destructive measurements. On the other hand, destructive methods can provide more accurate information about the crack volume and structure but cannot easily be combined with

R.D. Stewart, Crop and Soil Environmental Science Dep., Virginia Tech, Blacksburg, VA 24060; M.R. Abou Najm, Civil and Environmental Engineering, American Univ. of Beirut, Beirut 1107 2020, Lebanon. *Corresponding author (rds@vt.edu).

Methods of Soil Analysis
2017, Vol. 2
doi:10.2136/msa2015.0043

Received 5 Sept. 2016.
Accepted 10 May 2017.

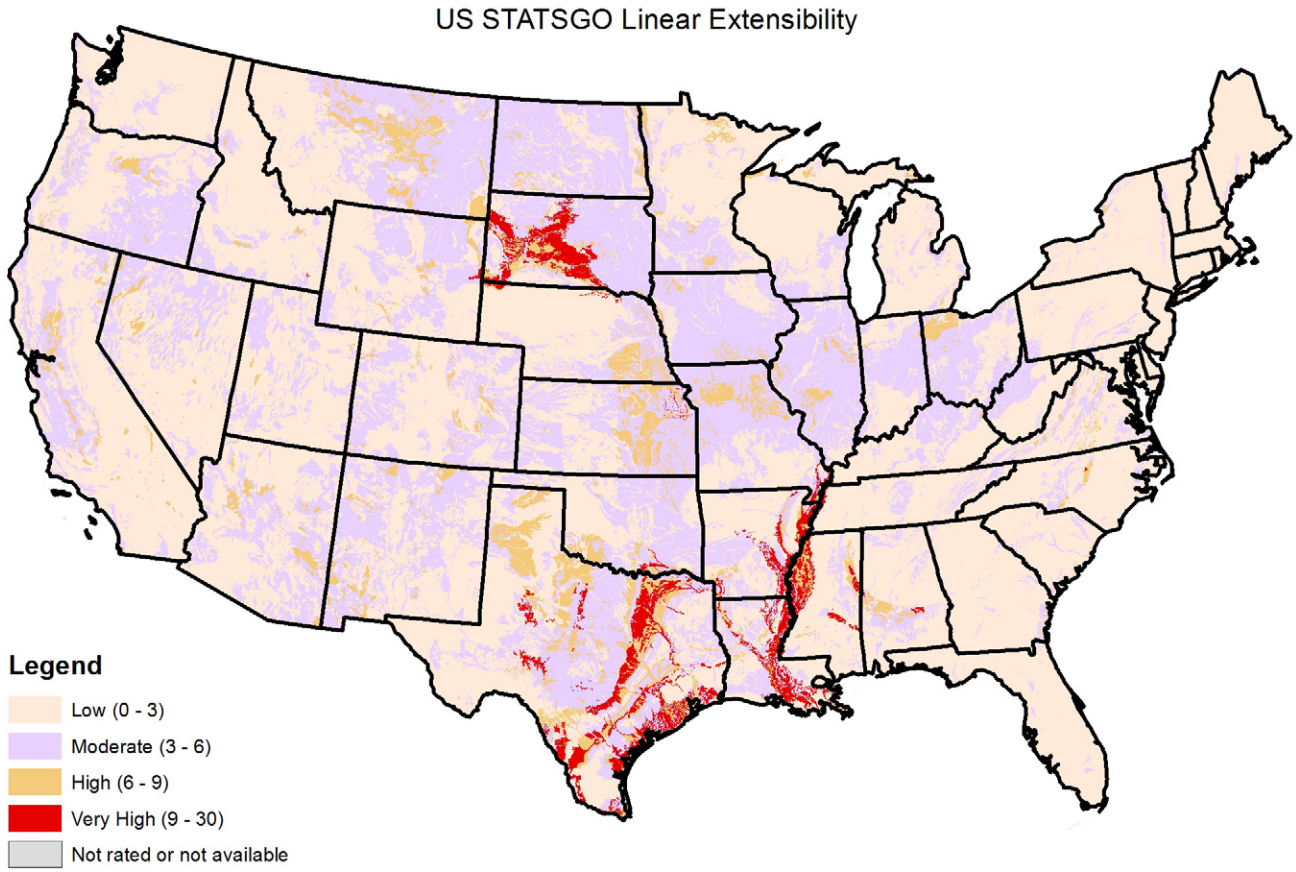

Fig. 1. Map of linear extensibility values for soils of the United States based on surface layer properties (depth-weighted average of the upper 1 m) in the USDA STATSGO database.

complementary or repeated measurements. Here we review the most common or promising methods in each category.

Nondestructive Methods

The most common method to determine crack volumes relies on physically measuring the crack widths and depths and then assuming a characteristic geometry. Crack widths are typically quantified using a measuring tape (Ringrose-Voase and Sanidad, 1996; Favre et al., 1997; Kishné et al., 2009), although calipers (Návar et al., 2002) or V-shaped gauges (Zein El Abedine and Robinson, 1971) have also been used. Crack depths are then estimated using some sort of flexible, pointed tape (Miller et al., 2010), ruler (Ringrose-Voase and Sanidad, 1996), or rod (Zein El Abedine and Robinson, 1971). In a recent variation, Greve et al. (2010) used a lighted fiberglass video-scope probe to measure crack depth while simultaneously providing images of subsurface structure, although that method was constrained to large cracks (>8-mm width).

To determine the total crack volume, the crack geometry must be assumed. The typical assumption is that cracks are triangular in shape (Zein El Abedine and Robinson, 1971; Elias et al., 2001), although mature cracks may be better described as rectangular or parabolic in shape (Ringrose-Voase and Sanidad, 1996). Regardless of the geometry selected, significant errors can occur with this method because it captures very little about the subsurface features of the crack. For example, any tortuosity or deviation from the vertical direction can cause refusal of the depth probe, thus providing an underestimate of the actual depth.

Despite its potential inaccuracy, these physical measurement methods are repeatable and use commonly available, inexpensive equipment. Although time consuming, this method can be used for multiple cracks within a landscape and thereby provide an indication of spatial variability. Likewise, the measurements can be repeated on the same cracks with time, thereby providing quantitative information on changes in crack structure because of some alteration (e.g., irrigation). On the other hand, the method is labor intensive, relies on simplistic geometric assumptions to calculate volumes, and does not capture subsurface crack complexity or connectivity.

Other recent methods have been developed that add various degrees of automation to the measurement process. In one example, Favre et al. (1997) developed a 3:1 strain gauge system that is inserted into the soil, spanning a crack. The relative motion of the crack walls due to shrinkage and swelling can then be accurately measured by reading the change in gauge width. In another example, Stewart et al. (2015) used digital imaging to quantify changes in the surface area of cracks with time in response to controlled irrigation. Both methods can be augmented with crack depth probe measurements, e.g., Miller et al. (2010), to fully characterize representative cracks with time.

In an attempt to directly measure relative changes in crack volumes, Stewart et al. (2012) developed a displacement-based

instrument that is installed directly into a representative crack (see below). In its most basic configuration, the instrument consists of a bladder (inserted into the crack) that is filled with water or a similar fluid. The bladder is then connected to a standpipe in which the water level changes in response to changes in the crack volume. This instrument is ideal for observing dynamic variations in crack volume but, like most nondestructive measurements, provides little information about the connectivity and complexity of crack networks. Moreover, the continued presence of the water-filled bladder may cause soil deformation and influence subsequent crack patterns, thus affecting long-term measurements.

In a different approach, researchers also have measured changes in surface elevation due to shrinkage and swelling and then, by assuming a shrinkage geometry factor, can predict crack volumes given the amount of surface subsidence. The vertical changes in height are typically measured using a benchmark that is attached to a deeper, non-swelling layer, thus providing a consistent datum (Bronswijk, 1991). Ground anchors can then be affixed to the soil profile at various depths, such that the relative swelling of different layers and horizons can be evaluated relative to the benchmark (te Brake et al., 2013). As an alternative, Neely et al. (2014) developed a system in which magnets are placed at various depths in the soil profile external to an access tube; the vertical position of the magnets relative to the soil surface can then be measured by passing a magneto-resistive sensor down the access tube. This magnet position sensor provides an easier installation than the ground anchor system and allows the soil water content to be measured with a neutron probe in the same location.

Finally, crack dimensions can be inferred from hydraulic measurements of the soil, typically using some form of tension infiltrometer experiment (Lin et al., 1998; Zhang et al., 2014). Specifically, the tension infiltrometer instrument can be set at multiple tensions, and proportional changes in infiltration rate can then be attributed to specific pore size classes whose size can be inferred using capillary theory (Watson and Luxmoore, 1986). Such measurements are repeatable in both time and space, although they may not be appropriate for larger (wider) cracks due to the breakdown of the Poiseuille or Darcian flow (Germann and Karlen, 2016), as well as the effects of complex pore geometry and topology on saturated hydraulic conductivity measurements (Hunt, 2001).

Destructive Methods

In contrast to the nondestructive methods covered above, destructive methods generally are used to obtain single (typically more detailed) measurements of crack volumes, after which time the soil structure is irrevocably altered. Destructive methods provide more detail on the pore structure and its connectivity than those obtained from nondestructive methods. In our present discussion, we focus on methods that quantify the properties of surface-connected cracks, noting that with careful excavation (e.g., using an auger borehole) it may be possible to use many of the following destructive methods to examine crack networks at depth.

The most common destructive methods involve filling cracks with various substances, including white cement (Neely, 2014), plaster of Paris (FitzPatrick et al., 1985), liquid latex (Abou Najm et al., 2010), hardening resins (Cabidoche and Ruy, 2001; Shipitalo et al., 2004), and sand (Dasog and Shashidhara, 1993). In general, the total volume of substance required to fill one or more cracks is measured. However, in the case of hardening fluids such as liquid latex, resins, and cements, the casts can be extracted from the soil after setting, thereby enabling the quantification of crack volumes via laser scanning or fluid displacement measurements (Jabro and Iversen, 2015). Analysis of extracted casts can provide additional quantitative information about the crack profile (e.g., geometry) and complexity (e.g., connectivity).

Non-Newtonian (e.g., shear-thickening) fluids, such as guar gum, xanthan gum, and methyl cellulose, have also been tested to measure crack volumes (Stewart et al., 2014). These specific thickening agents are biodegradable, which means that with time they will be consumed by microorganisms. While the exact interactions between microbes and such shear-thickening substrates have not yet been studied in the context of shrink–swell soils, in theory the addition of any of these substances to a crack network may be considered to be nondestructive relative to the casting agents. However, there are some difficulties in applying these substances to a crack network, given that some finite amount of the fluid will infiltrate into the soil matrix itself and that it can be difficult to discern when the substance has fully filled the crack. More recently, Abou Najm and Attalah (2016) presented a new theoretical framework that uses infiltration experiments with multiple non-Newtonian (shear-thinning) fluids to decipher the effective size and corresponding flow contribution of multiple representative pore radii. So far, the method was validated only with synthetic porous materials but has shown potential for use in pore structure characterization.

Overall, both nondestructive and destructive methods can provide quantitative assessments of crack dimensions, albeit with different sets of assumptions and limitations. The choice of which method to use ultimately depends on the focus and constraints of any particular study. For this reason, we have elected to recommend three different methods that we consider best able to capture soil crack dimensions at reasonable accuracy with high spatial or temporal resolution: the tape and rod method, the displacement method, and the cast and excavate method.

EXPERIMENTAL PROCEDURE

Identification of Representative Cracks and Surface Areas

Vertic soils can display substantial heterogeneity in the size of individual cracks and of soil peds that exist between cracks. The following methods are best utilized on areas much larger than an individual crack or ped, so a preliminary survey is recommended for any field application focused on measuring crack properties. Figure 2 shows a 32- by 45-cm frame with three 2.5-cm, three 5.0-cm, and three 10.0-cm rings demonstrating the range of possible errors that may occur from adopting a small and non-representative surface area. We present below a methodology to identify a representative crack or surface area for the application of any of the proposed crack characterization methods.

Methodology

To perform the preliminary survey, we propose that a minimum of six random locations should be chosen within the site (more may be required for studies occurring across large

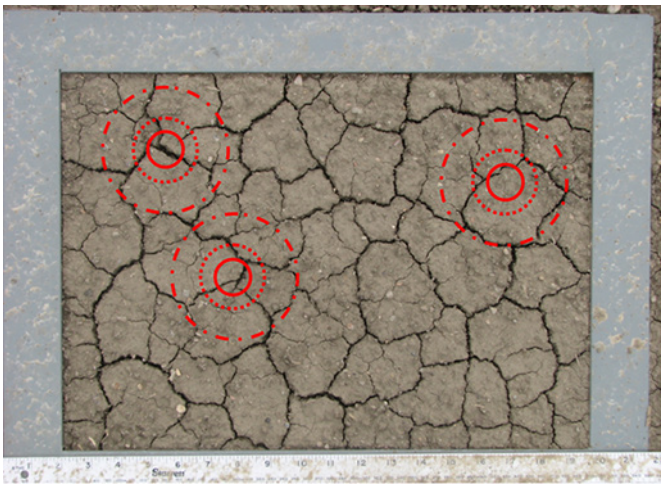

Fig. 2. A 32- by 45-cm imaging frame showing the range of possible errors that may occur from adopting a small and non-representative surface area. The smallest rings are 2.5 cm in diameter, the middle rings are 5.0 cm in diameter, and the largest rings are 10.0 cm in diameter. The ruler is in inches.

spatial extents or sites that exhibit high variability in their cracking patterns). At each location, any vegetation should be carefully removed or cropped down to the surface. A large (e.g., 32- by 45- or 50- by 50-cm) frame should then be placed on the soil surface. When possible, digital image analysis can be used to extract two-dimensional cracking characteristics including distributions of ped areas and perimeters as well as crack widths and lengths. When such level of detail is not desired, simpler methods can be utilized. In either case, researchers can identify the number of individual soil peds (defined here as the masses of soil that are bordered by cracks) that are captured within the frame, counting each ped that is wholly contained within the frame as one and each ped that passes the perimeter as one-half. When one or more edges of a ped are difficult to decipher, it is recommended that each ped be constrained using a simple geometric shape (e.g., square, hexagon, rectangle, or triangle), making sure that those shapes cover the full extent of the frame (e.g., Fig. 3). The average soil ped area can then be calculated as the frame area (e.g., 50 ´ 50 cm = 2500 cm^2) divided by the number of peds. In the example of Fig. 3, the 2500-cm^2 frame has captured approximately six complete peds (orange boxes) and approximately 12 incomplete peds (purple boxes). This means that the frame includes approximately 12 peds (6 + 12/2 = 12), and the average ped area is approximately 210 cm^2 (2500 cm^2/12 = 210 cm^2). We recommend the adoption of this process at all sampling locations, after which time an overall mean and standard deviation can be calculated for the site, thus allowing sizing of a reasonable representative area. The measurement size required for any of the following methods (e.g., cast and excavate) should then be designed to be at least 10 times the mean soil ped size.

If information about crack dimensions are desired, for example if attempting to select a crack with representative dimensions for detailed measurements or monitoring, then a preliminary crack survey should be conducted using the tape and rod method, as quantified in the following section. This will enable the practitioner to quantify the size (e.g., width and depth) of cracks within the site and select representative cracks appropriately.

Fig. 3. Division of a 50- by 50-cm sampling frame into soil peds that are surrounded by cracks, which can be used to estimate the approximate average size of the peds. Orange boxes denote peds that are fully within the frame, while purple boxes represent peds that are partially within the frame.

Tape and Rod Method

The first recommended method involves the physical measurement of the width and depth of multiple cracks along one or more transects. While the length (i.e., longitudinal distance) of the cracks can also be estimated in this method, the fragmented and nonlinear nature of crack propagation often makes this a challenging endeavor. Instead, as shown in the calculations, it is generally preferable to calculate crack length densities and volumes on a per area basis.

Required Supplies

This method requires an accurate measuring tape (steel or cloth) for measuring horizontal crack dimensions and a thin metal rod for estimating crack depths. Flexible cloth tapes have the advantage of being able to conform to the general shape of a crack, which can be important for determining the longitudinal extent of cracks (if desired). For depth determinations, 1/16″ (0.16-cm) diameter stainless steel rods can be obtained at lengths up to 2 m. Such rods are flexible yet strong enough to be inserted deep into the crack. Individual rods can be marked or scored with distance markings to facilitate measurement readings.

Methodology

As with the other recommended methods, the tape and rod method works best if the cracks are exposed (i.e., free of any thick vegetation). Thus, any vegetation should be closely cropped before commencing the measurements. Once the site is properly prepared, the first step of the analysis requires the establishment of measurement transects at the sampling site. This can be accomplished using a complete survey of the area and measuring all cracks encountered, or by sampling

cracks along one or more transects. In the case of the transect approach, Ringrose-Voase and Sanidad (1996) recommended using a series of linked semicircles, which can help avoid measurement bias due to preferential orientation of cracks (Fig. 4). The general procedure for setting out a transect is as follows:

1. Choose a starting location for the transect and mark it with a stake.
2. Using a string and another stake, mark out a straight line in the direction of the transect.
3. Using additional stakes, mark every 1 m (or desired measurement interval) along the length of the string.
4. Lay a semicircle measurement pattern between the first and second positions (stakes) on the transect string. Note that a semicircle measurement pattern can be physically constructed from stiff wire and a 1-m piece of wood or pipe.
5. Moving along the semicircle arc, count all cracks wide enough to accommodate the depth rod. At each crack, measure the crack width, W_i, and depth, D_i. Record these measurements.
6. After reaching the other end of the semicircle arc, the semicircle is moved so that its ends now rest between the second and third stakes. Note that the direction of the arc should be opposite of the original position so as to form an "S" shape (see Fig. 4). Continue counting the number of intercepting cracks along the arc.
7. Repeat Step 6 until a sufficient number of cracks (generally >50) have been identified and measured, making sure to count all cracks that intersect the final semicircle. The total number of intercepted cracks, N, is recorded along with the total number of semicircles that were used, M.
8. In the case that a linear (rather than semicircular) transect is used, it is advisable to also measure the width and depth of the crack at some distance (e.g., 20 cm) in both directions from the intersection point, which will allow better averaging. At a minimum, width and depth measurements should be taken at least three times for every linear meter of crack length.
9. To quantify the temporal evolution of the cracks, the measurement protocol can be repeated as often as desired. However, care should be taken to avoid excess foot traffic on the site due to the high potential for compaction and erosion that can occur as a result.

Note that for well-exposed cracks, digital imaging can also be used to quantify the surface crack area (i.e., width and length); the image collection and analysis procedures are described in detail for the cast and excavate method below.

Calculations

Once the measurements have been completed, an estimate of the length of cracks (L_c) found within some given area (A) can be found using the equation derived by Newman (1966):

$$L_c = \frac{\pi N A}{2 L_t} \qquad [1]$$

where N is the number of intersections between the crack(s) and lines, with a total length L_t, that have been placed within the area. If we assume L_t is the total length of semicircles inscribed across the transect, then the crack length per unit area of soil surface (i.e., the crack length density, L_A [L L^{-2}]) can be calculated as

$$L_A = \frac{L_c}{A} = \frac{\pi N A}{2 L_t A} = \frac{\pi N}{2 L_{sc} M} \qquad [2]$$

where L_{sc} is the length of the semicircle used. If a 1-m-diameter semicircle is used, then $L_{sc} = \pi/2$ m and Eq. [2] simplifies to $L_A = N/M$ (Ringrose-Voase and Sanidad, 1996).

Similarly, the mean crack width, $\overline{W}$ [L], and depth, $\overline{D}$ [L], can be calculated by

$$\overline{W} = \frac{1}{n}\sum_{i=1}^{n} W_i \qquad [3]$$

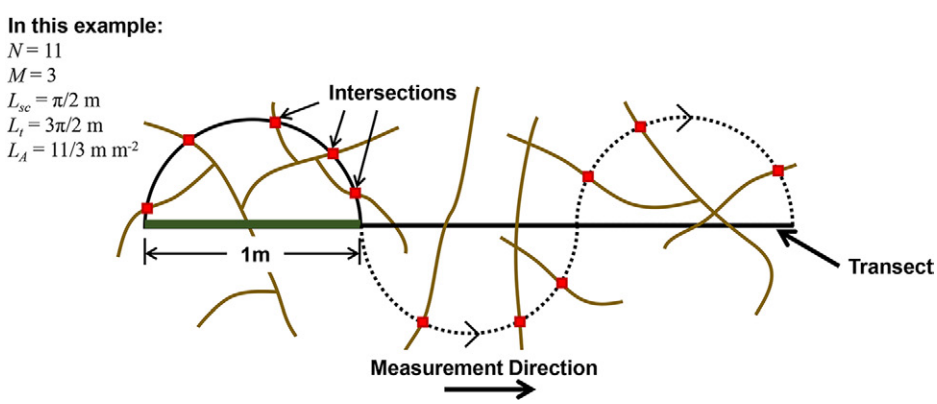

Fig. 4. Schematic for laying out a transect for physical crack measurement (e.g., using the tape and rod method), as recommended by Ringrose-Voase and Sanidad (1996). A semicircle (1-m diameter) is laid out on the transection, and all cracks that intercept the hoop (indicated by red squares) are measured for their widths and depths at the interception location. The semicircle hoop is then placed along the dotted lines until the end of the transect is reached. In this example, the number of intercepts N = 11, the number of semicircles M = 3, the diameter of the semicircle = 1 m, the length of the semicircle L_{sc} = p/2 m, the total length of the semicircles along the transect L_t = 3p/2 m, and the crack length density L_A = 11/3 m m^{-2}.

$$\bar{D} = \frac{1}{n}\sum_{i=1}^{n} D_i \quad [4]$$

where n is the number of intercepts measured (which may differ from the number of intercepts counted, N).

By assuming a geometric form for the cracks, the widths (W_i) and depths (D_i) that are measured at the soil surface can be used to determine additional properties. These properties include the change in crack width as a function of crack depth, $w(d)$ [L], the cross-sectional area of the crack, X [L^2], and the boundary length, B [L], which represents the length of the soil–atmosphere interface in the vertical plane (Fig. 5). We focus here on three crack geometries that were discussed by Ringrose-Voase and Sanidad (1996): rectangular, triangular, and parabolic (where the crack width has a square root relationship with depth).

In the case of a rectangular crack, the measured width W is assumed to be constant for the entire depth profile, i.e., $w(d) = W$. For a triangular crack, width can be predicted as

$$w(d) = \frac{W}{D}(D-d)$$

while for a square-root parabolic crack, width can be found by

$$w(d) = \frac{W}{D^{1/2}}(D-d)^{1/2}$$

Note that d represents the vertical distance from the crack surface [L].

Next, the mean cross-sectional area of the cracks, $\bar{X}$ [L^2], can be found by

$$\bar{X} = \frac{1}{\lambda n}\sum_{i=1}^{n}(W_i D_i) \quad [5]$$

where λ is a parameter that depends on the assumed crack geometry. Note that $\lambda = 2$ for a triangular cross-section, $\lambda = 1.5$ for the square-root parabola, and $\lambda = 1$ for a rectangular cross-section.

The mean crack volume per unit area, $\bar{V}_A$ [$L^3\ L^{-2}$], can be quantified as

$$\bar{V}_A = \bar{X} L_A \quad [6]$$

The crack dimensions D_i and W_i can also be used to compute the boundary length of each crack, B_i [L], representing the length of the crack exposed to the atmosphere (i.e., the length of its exposed face in the vertical plane). The boundary length for a triangular crack can be calculated as

$$B_i = 2\sqrt{(W_i/2)^2 + D_i^2} \quad [7]$$

while for a parabolic cross-section (where width is proportional to the square root of depth) by

$$B_i = \frac{W_i}{2}\left(\sqrt{1+\frac{16D_i^2}{W_i^2}}\right) + \frac{W_i^2}{8D_i}\ln\left(\frac{4D_i}{W_i} + \sqrt{1+\frac{16D_i^2}{W_i^2}}\right) \quad [8]$$

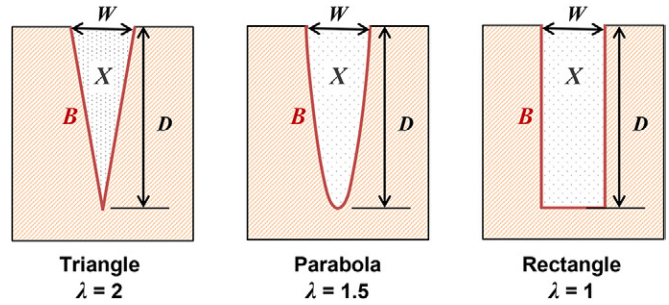

Fig. 5. Examples of possible crack geometries for cracks of width W and depth D that can be assumed when determining cross-sectional area X and boundary length B (i.e., the length of crack surface exposed to the atmosphere in the vertical plane, as indicated by the heavy red line between the soil and crack). The geometry-dependent factor λ (Eq. [5]) changes with the assumed crack geometry.

and for a rectangular cross-section by

$$B_i = 2D_i + W_i \quad [9]$$

Finally, the mean surface area per unit area of cracks exposed to evaporation, $\bar{S}_A$ [$L^2\ L^{-2}$], can be determined on a per unit area basis by multiplying the mean boundary length by the crack length density, L_A:

$$\bar{S}_A = \frac{L_A}{n}\sum_{i=1}^{n} B_i \quad [10]$$

Displacement Method

A second recommended method is to physically install sensors into the cracks to determine volume change dynamics at high temporal resolution. Note that this method is best suited to quantify relative changes in crack volume and should be combined with the tape and rod method to determine absolute volumes. Stewart et al. (2012) developed a displacement-based instrument (termed the "crack-o-meter") that can, for the most part, be constructed from common components found at a hardware store. The system is comprised of a bladder that is inserted into a crack and then connected to a standpipe (Fig. 6). Water is added to the standpipe until the bladder is filled and a slight positive pressure head is maintained above the connection point.

Required Supplies

- flexible bladder, which can be fashioned from intravenous (IV) bags (e.g., Braun Corporation) or hydration pack bladders (e.g., Cascade Designs, Inc.)
- 3-cm (1–1/4 inch) diameter polyvinyl chloride (PVC) pipe (200-cm length per installation)
- 3-cm-diameter PVC cap (two required)
- 0.6-cm (1/4 inch) barbed hose fitting
- 0.6-cm plastic hose
- PVC cement
- Teflon tape

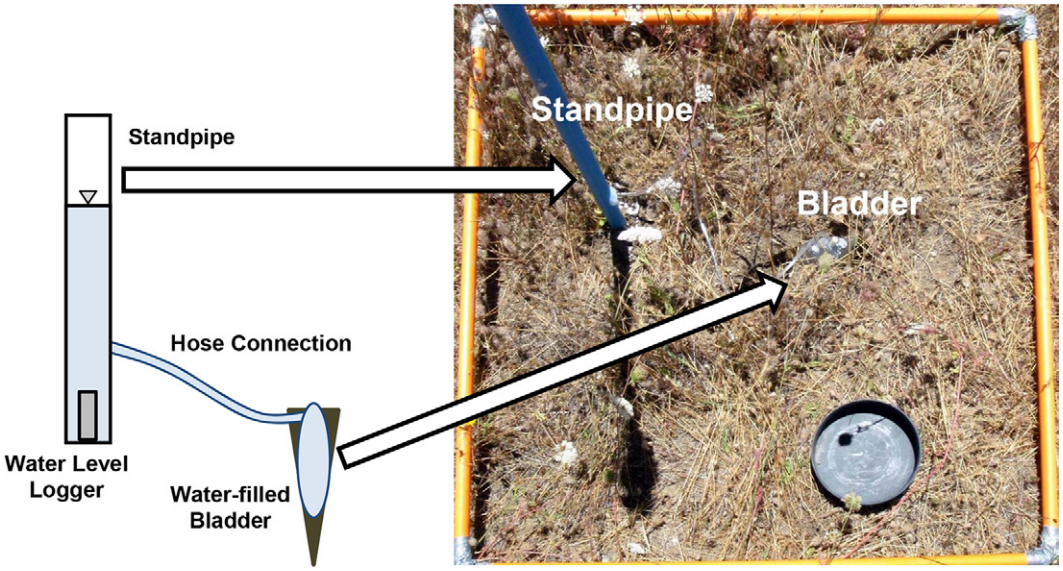

Fig. 6. Example usage of a displacement sensor (right), and components of the displacement sensor, in which water moves between a water-filled bladder placed within the crack and a standpipe where the water level is recorded (left).

- 3-cm-diameter PVC Tee (optional)
- PVC reducing hardware to connect PVC Tee to 0.6-cm barbed hose fitting (optional)

Methodology

The displacement instrument is constructed using the following steps:

1. Using PVC cement, glue one of the 3-cm-diameter PVC caps to one end of the 3- by 200-cm PVC pipe.
2. Once the cement has cured, affix the barbed hose fitting to the PVC pipe. The fitting should be located approximately 40 cm from the end of the pipe with the glued-on cap. The fitting can be attached either by drilling and tapping (i.e., threading) a hole directly into the pipe or by cutting the PVC pipe at this location and attaching both ends (using PVC cement) to the optional 3-cm PVC Tee. Note that if a Tee is used the pipe sections should be attached to either end of the long dimension of the Tee, and reducing hardware should be used to attach the barbed hose fitting to the short dimension of the Tee. In either case, Teflon tape should be used around the threads of the barbed fitting to ensure a water-tight seal. Once constructed, the standpipe system should be oriented vertically (i.e., with the glued PVC cap end of the pipe pointing down) and filled with water to verify that the connections are watertight.
3. Using a 5-cm (2 inch) hand auger, dig a hole adjacent to the crack to be measured. The hole should be ~35 cm in depth and should be located a minimum of 25 cm from the crack face.
4. Place the capped end of the PVC pipe into the hole and backfill as necessary. The standpipe should be firmly placed in the soil.
5. The empty bladder should be carefully inserted into the crack. Wire or another thin yet solid material can be useful to guide the bladder into position, so long as care is taken to avoid puncturing the bladder.
6. After the bladder is placed, an appropriate length of rubber hose is used to attach the bladder to the barbed hose fitting.
7. Water is then added to the bladder via the standpipe. The bladder should expand to fill the width of the crack, at which time the water level within the standpipe should begin to rise above the connection point. In general, a water level of 15 to 20 cm above the connection point will suffice. While filling the bladder, care should be taken to ensure that air bubbles do not become trapped in the bladder or connecting hose. This may necessitate disconnecting the hose and purging air bubbles at the connection points.
8. The water level within the standpipe can be measured manually using level tapes or automatically using conductance water levels or sealed or vented pressure transducers. These choices represent tradeoffs between measurement frequency, measurement accuracy, and cost; it is up to the researcher to decide which method is preferable for any given application.

Note that while the displacement instrument is well suited for measuring dynamic changes in soil volumes, the continued installation of the bladder may cause eventual deformation and degradation of the surrounding soil. In particular, the bladder will act as a weak point from which cracks will propagate during drying phases. At the same time, the bladder material will weaken with time. Thus, such instruments should be inspected and moved to new locations at regular intervals to ensure the continued quality of the data. Note also that this method is biased toward larger cracks due to the necessity of installing the bladder from the surface. The other recommended methods (and in particular the cast and excavate method) are better suited for sampling the entire range of pore sizes.

Calculations

Changes in crack volume, ΔV, can be calculated from relative changes in water level within the standpipe Δh:

$$\Delta V = \pi r^2 \Delta h \qquad [11]$$

where r is the internal radius of the standpipe.

The mean change in the crack width for the portion of the crack that is in contact with the bladder (Δw^*) can then be calculated as

$$\Delta w^* = \frac{-\pi r^2 \Delta h}{YZ} \qquad [12]$$

where Y is the effective length and Z is the effective depth of the bladder (i.e., the respective horizontal and vertical contact lengths between the bladder and the soil). Note that if the crack has a rectangular geometry, then Δw^* equals the mean change of width for the total crack (ΔW). In the case of a triangular crack, the mean change in total crack width can be found by

$$\Delta W = \frac{\Delta w^*}{2\left(1 - Z/2D\right)}$$

where D is the total depth of the crack.

Cast and Excavate Method

The cast and excavate method starts with a choice of casting fluid, which will vary based on application, budget, and complexity of the pore network. Several casting materials have been previously used including white cement (Neely, 2014), plaster of Paris (FitzPatrick et al., 1985), liquid latex (Abou Najm et al., 2010), hardening resins (Cabidoche and Ruy, 2001; Shipitalo et al., 2004), and sand (Dasog and Shashidhara, 1993). Some applications require only estimates for the total volume of cracks or pores (for example, earthworm channels), in which case filling the void with a measured quantity of a substance such as plaster of Paris, gypsum, or sand should suffice. Other applications may be more demanding in terms of maintaining the form of the pore structure to study its connectivity and shape; in such cases, fluids like liquid latex or resins may be used.

In this context, Abou Najm et al. (2010) showed the ability of liquid latex to infiltrate through the complex interconnected pore structure and fill the pores classified as preferential flow paths with very limited infiltration into the soil matrix. This casting material was therefore shown to be capable of separating the pore structure into (i) surface-connected preferential

Fig. 7. Examples of different crack networks obtained using liquid latex. Additional details were provided by Abou Najm et al. (2010).

flow paths and (ii) soil matrix pores (Fig. 7). After drying and hardening, the mold can be extracted, enabling three-dimensional visualization of the surface-connected preferential flow paths. One limitation to this method is its inability to detect preferential flow paths that are not connected to the surface (because liquid latex does not infiltrate the matrix pore structure); however, it may be possible via careful excavation of the overburden layer (e.g., using a hand auger) to intercept subsurface cracks, at which point the latex can be added.

Required Supplies

- liquid latex
- imaging frame of appropriate size (e.g., constructed using 1.2-cm [1/2 inch] diameter PVC)
- digital camera
- spade or similar tools to excavate latex cast (see Step 5 below)

Methodology

The following steps are adopted from the methodology proposed by Abou Najm et al. (2010), where liquid latex was the casting fluid, but can be extended to include other fluids (e.g., white cement or gypsum) or amended to fit different applications.

1. **Selection of a representative surface area:** Different cracking patterns are observed for different soil types, land covers, water table depths, and moisture contents. Such patterns span the full spectrum from being linear at the row center, as observed in row-planted corn (*Zea mays* L.) fields, to forming classic multisided peds. Once a reasonable representative dimension is selected (see above for more information on how to select representative areas), a minimum of three areas (frames) should be laid out for sampling. Note that if extreme differences are observed in the volumes of latex needed for each frame (e.g., more than a factor of 10), additional frames may be required to accurately capture site heterogeneity.
2. **Surface preparation:** A frame to confine the representative surface area is placed at the surface before pouring the latex. The frame material should ideally be metal or PVC (or any material that does not swell). To ensure that latex does not spill out of the frame area, soil at the surface must be in close contact with the frame and all openings between the frame and the soil surface should be sealed with repacked (typically wet) soil to ensure proper contact.
3. **Field characterization:** Taking one or more digital images of the frame before pouring the latex can be very helpful in subsequent interpretation of crack orientation, etc. In addition, field bulk density and water content can be measured at multiple depths via collection of undisturbed soil samples (from outside of the sampling frame).
4. **Casting:** Liquid latex must be poured slowly inside the cracks to provide the needed time for the latex to infiltrate through those preferential flow paths, thus allowing the latex to fill the crack(s). This process can last for more than an hour in deep and complex pore structures where latex infiltrates into deeper and smaller cracks. In this case, liquid latex can be added in small amounts every 1 or 2 min until the latex level within the entire frame stabilizes for at least 5 min. The latex will then require 8 to 12 h to solidify. Note that the liquid latex material used by Abou Najm et al. (2010) was a high-tear-strength latex rubber with 95% minimum recovery (hysteresis) and 60% total solids.
5. **Excavation:** Latex removal methods vary depending on the depth and connectivity or complexity of the cracking network. In shallow vertical cracks, the latex molds often terminate at depths of 5 to 10 cm with limited lateral expansion. Under such conditions, careful excavation using a shovel can be sufficient. To ensure no loss of any latex that may result from the shovel's cutting edge, a minimum of 15 cm of buffer around the frame is recommended. In deep and complex crack networks where the lateral and vertical extent of the latex is unknown, using a shovel for excavation may lead to the loss of much detail if the shovel's edge cuts some of the latex. Thus, a more careful excavation approach is needed and smaller tools (e.g., screwdrivers) may be utilized, although this typically increases the time required for excavation (e.g., up to 6–8 h for a 32- by 45-cm frame).
6. **Latex preparation:** Once excavation is completed and the latex frame is completely separated from the soil, the latex frame must be clean of all remaining soil. The top of the latex frame should then be attached in a rigid horizontal platform to prepare it for volume calculations.
7. **Volume calculations:** Jabro and Iversen (2015) presented a movable platform that lowers the latex frame at known increments into a fluid container and measures the increase in fluid level using a linear variable displacement transformer. They found that containing the fluid and measuring the increases in the water level performed better than measuring the volume of the displaced fluid (due to irregularities caused by surface tension of the water). Depth intervals (increments) can be determined based on crack depths and characteristics and typically range between 1 and 5 cm.

Lateral Cracks

Due to the complexity of pore structure, large cracks often extend underground laterally beyond the frame area (Fig. 7). The liquid latex method can be used to track the connectivity of such lateral preferential networks, thus providing qualitative understanding of the directionality and connectivity of such pore structures. However, when lateral cracks dominate, care should be taken when calculating crack volume per area or volume of soil. For example, the volume of a 100-cm-long lateral crack starting from a surface crack within a 32- by 45-cm frame cannot be attributed solely to the frame area. In such a case, the total volume of latex can be measured and then lateral cracks can be trimmed from the latex frame, which is then followed by a second volume measure. Combining both measurements can provide an indication of the pore structure.

Surface Roughness

The volume of latex in the top few centimeters (toward the surface) must be closely investigated because surface roughness may contribute to an increase in the latex volume. This volume must not be mistaken as being representative of

preferential flow paths. Abou Najm et al. (2010) suggested using a predefined upper threshold that can be estimated by the ratio of cracks at the surface to the total surface area. Note that this ratio can be calculated from digital image analysis of the surface image and typically does not exceed 10%. Thus, for a 32- by 45-cm frame with a surface layer height of 2 cm, any measured volume of latex exceeding 0.1 ´ 2 cm ´ 32 cm ´ 45 cm = 288 cm^3 would exceed the threshold of 10% and the excess volume should be removed from the analysis.

RECOMMENDATIONS

The choice of method will ultimately depend on the objectives and constraints of any given experiment. If a single crack volume value is required, the cast and excavate method offers the best accuracy and information about the structure and density of crack networks. However, as mentioned above, this method is generally destructive to the soil and so is not conducive to repeated or supplementary measurements.

For applications requiring dynamic measurements to capture the variability associated with time- or water-content-dependent dynamics in crack volumes, the tape and rod and displacement methods are recommended. The tape and rod method allows greater spatial coverage of a location, although with a tradeoff that the measurements can typically only be taken at relatively low temporal resolutions. The displacement method, conversely, offers high temporal resolution with limited spatial resolution. Therefore, the two methods can be considered complementary and may be used simultaneously for the best results. Here we note that both of these methods, and in particular the displacement method, are biased toward larger cracks due to the necessity of inserting physical objects (e.g., a displacement bladder or a measuring rod) into the cracks themselves.

If cost is a concern, the tape and rod method is generally the most affordable (notwithstanding the potential for high labor costs). The materials required to construct the displacement method instruments are generally inexpensive; however, automated measurement of the water level in the standpipe (e.g., with a pressure transducer and datalogger) will substantially increase the cost of an installation. Hand measurement of the water level can be an affordable alternative, although this will probably result in decreased measurement frequency compared with an automated system while also making the method more labor intensive. The overall cost of the cast and excavate method will vary widely, depending on the casting material used, the size of the area to be sampled, the connectivity of the pore structure, the total volume of the cracks, and whether or not heavy machinery will be required to excavate the material.

CASE STUDY

Crack Characterization during Infiltration and Runoff

As part of a plot-scale experiment to quantify hydraulic properties and hydrological processes for a hillslope characterized by soil cracks (Stewart et al., 2015), several of the aforementioned methods were used. The field site was located in the south-central portion of Chile, near the community of Ninhue (36°25′3.108″ S, 72°31′6.97″ W). During two consecutive summers (2011 and 2012), the plots were heavily irrigated and subsequent crack closure was measured using the displacement meters, manual measurements using the tape and rod method, and digital imaging on representative cracks.

Manual Measurements

Before the first irrigation event in 2011, crack dimensions for all visible cracks were measured throughout five different 3.5- by 11-m plots, using a tape measure for the width and approximate length and a pointed rod for the depth. A total of 117 cracks were measured for their lengths and widths; of those, 80 were also measured for depth. As seen in Fig. 8, the observed crack widths for all 117 cracks were well described using a lognormal distribution with a mean width of 0.5 cm (the geometric mean of the samples). The 80 fully characterized cracks were analyzed for their cross-sectional area X_i and boundary length B_i using Eq. [5] and [7–9].

The assumed crack geometry has some effect on the predicted cross-sectional area and volume (Fig. 9a), as predicted by the factor λ in Eq. [5]. In other words, the rectangular profile had the largest cross-sectional area (λ = 1), while the triangular profile was smaller by a factor of two (λ = 2) and the square-root parabolic profile was smaller by a factor of 1.5

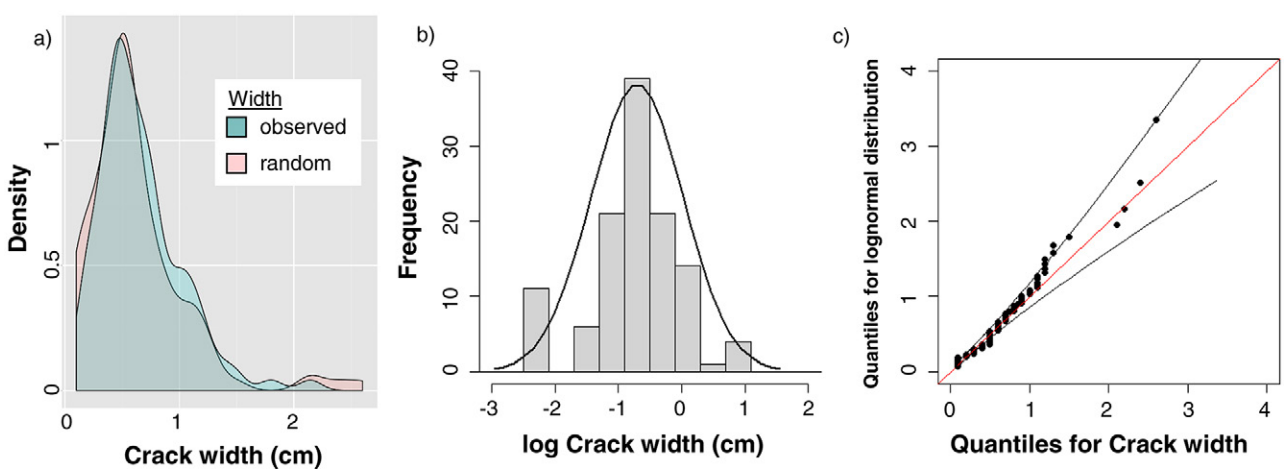

Fig. 8. Crack widths measured using the tape and rod method in a field site in south-central Chile, shown as: (a) measured distribution (red) compared with a lognormal distribution of random variables (green) that has a mean of 0.5 cm; (b) histogram of log crack widths fitted with a normal distribution; and (c) *q–q* plot showing the quantiles for measured crack width compared with the quantiles for a lognormal distribution.

(λ = 1.5). The calculated boundary lengths, on the other hand, were nearly identical regardless of geometry (Fig. 9b). The cracks surveyed in this example had much greater depths than widths (for example, the mean crack width was 0.5 cm, while the mean crack depth was 10 cm). As seen in Eq. [7–9], the boundary length for all three geometries will converge to $B_i \approx 2D_i$ if $D_i >> W_i$. Therefore, for narrow and deep cracks, crack geometry has only a minor effect on the calculated parameters, whereas for shallow and wide cracks, the choice of geometry becomes more important.

Displacement Measurements

In 2012, displacement instruments were installed into eight large cracks before irrigation. In addition, 50- by 50-cm quadrats were placed around 13 cracks, including one of the cracks that had a displacement instrument within it. The displacement sensors were set to record the water level every 3 min, while the quadrats were digitally imaged using a digital Pentax K-x digital single-lense reflex (dSLR) camera from a height of 60 cm. Images were collected before and after each discrete irrigation event, for a total of 8 to 12 images per crack.

Here we present data from the crack that was measured using both technologies (Fig. 10). For the displacement method, the measured water levels within the standpipe, $h(t)$, were converted to changes in crack width with time, $W(t)$, by assuming a rectangular crack geometry and by modifying Eq. [12] as

$$W(t) = W_0 + \frac{\pi r^2 \left[h_0 - h(t)\right]}{YZ} \qquad [13]$$

where W_0 is the initial crack width, r is the radius of the standpipe, and h_0 is the initial water height in the standpipe. Note that h_0 and $h(t)$ are defined as being positive upward, such that during the swelling process $h(t) \geq h_0$ as water is forced from the bladder into the standpipe. In this example, Y = 27 cm, Z = 7 cm, r = 1.6 cm, W_0 = 0.9 cm, and h_0 = 97.5 cm.

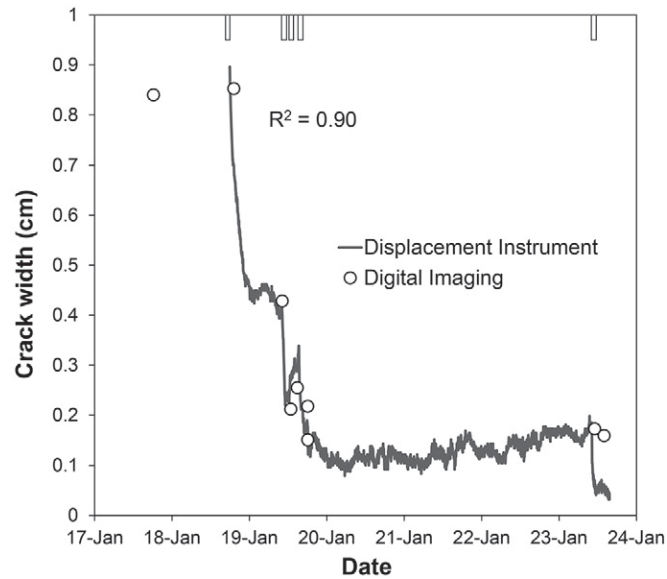

Fig. 10. Comparison of crack width W estimated from the displacement instrument placed within the crack vs. the crack width estimated from digital images taken from above the crack. The bars at the top of the frame indicate irrigation events.

The digital images were converted to grayscale and then renormalized using a custom MATLAB script so that the crack became represented by black pixels and the remainder of the area within the quadrat became represented by white pixels. The number of black pixels was then used to determine the crack area, A_c. The crack length L_c within the imaging frame was assumed to be constant, so that the crack width $w(t)$ can be determined as $w(t) = A_c/L_c$. In this example, the visible crack length L_c was taken to be 35 cm.

As seen in Fig. 10, these two methods correspond closely to one another, with an R^2 value of 0.90 and a root mean square deviation (RMSD) value of 5.3×10^{-3} cm. Both methods

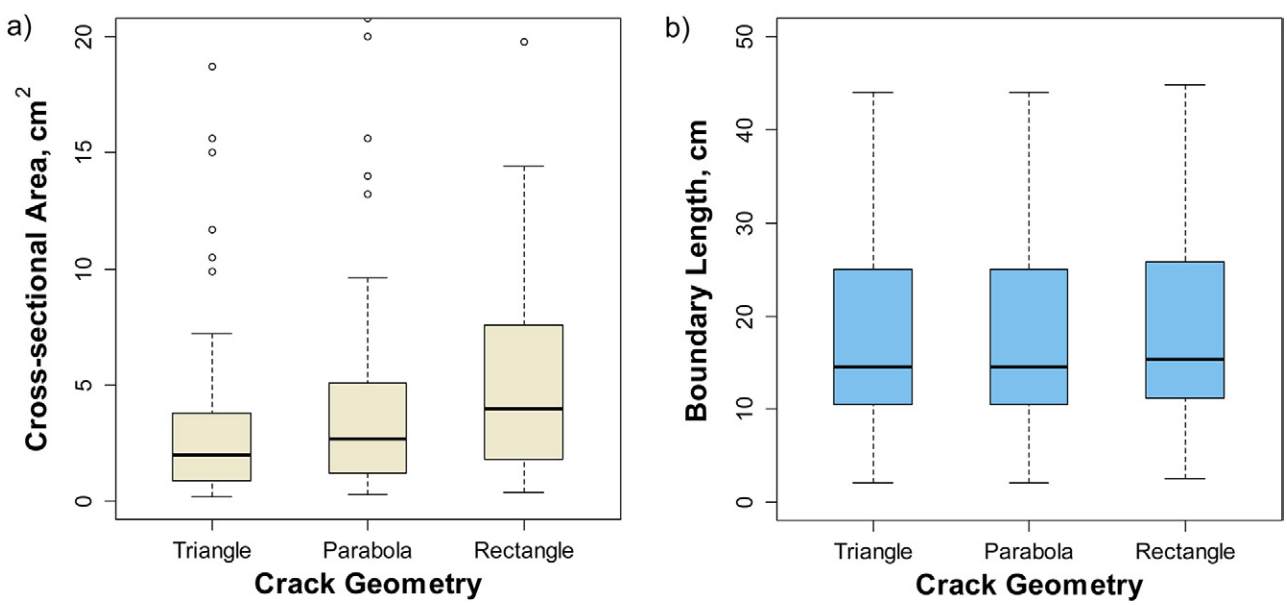

Fig. 9. (a) Cross-sectional area X (cm2) and (b) boundary length B (cm) for cracks measured at the example field site using the tape and rod method and assuming triangular, parabolic, and rectangular geometries.

captured the general trend that the crack became sealed as the plot was irrigated during a period of 6 d. The displacement measurement provided near-continuous data during the period, thereby revealing the swelling dynamics during different irrigation events.

CONCLUSIONS

By acting as preferential flow paths, shrinkage cracks often affect the movement of water, solutes, soil particles, and gases. Knowledge about crack sizes (e.g., width and depth) is thus needed to predict flow and transport processes through shrink–swell soils. The methods discussed here (rod and tape measurements, displacement sensors, and cast and excavate methods) each provide their own set of advantages and drawbacks. While no single method is capable of accurately and repeatedly characterizing crack features (e.g., volume, subsurface connectivity) in both time and space, a combination of these approaches can be used to improve understanding of crack dynamics and variability. Altogether, the methods surveyed here should enable practitioners to quantify the characteristics and behaviors of soil cracks.

REFERENCES

Abou Najm, M.R., and N.M. Attalah. 2016. Non-Newtonian fluids in action: Revisiting hydraulic conductivity and pore size distribution of porous media. Vadose Zone J. 15(9). doi:10.2136/vzj2015.06.0092

Abou Najm, M.R., J.D. Jabro, W.M. Iversen, R.H. Mohtar, and R.G. Evans. 2010. New method for the characterization of three-dimensional preferential flow paths in the field. Water Resour. Res. 46:W02503. doi:10.1029/2009WR008594

Bronswijk, J.J.B. 1991. Relation between vertical soil movements and water-content changes in cracking clays. Soil Sci. Soc. Am. J. 55:1220–1226. doi:10.2136/sssaj1991.03615995005500050004x

Cabidoche, Y.-M., and S. Ruy. 2001. Field shrinkage curves of a swelling clay soil: Analysis of multiple structural swelling and shrinkage phases in the prisms of a Vertisol. Soil Res. 39:143–160. doi:10.1071/SR99132

Dasog, G.S., and G.B. Shashidhara. 1993. Dimension and volume of cracks in a Vertisol under different crop covers. Soil Sci. 156:424–428. doi:10.1097/00010694-199312000-00007

Elias, E.A., A.A. Salih, and F. Alaily. 2001. Cracking patterns in the Vertisols of the Sudan Gezira at the end of the dry season. Int. Agrophys. 15:151–155.

Favre, F., P. Boivin, and M.C.S. Wopereis. 1997. Water movement and soil swelling in a dry, cracked Vertisol. Geoderma 78:113–123. doi:10.1016/S0016-7061(97)00030-X

FitzPatrick, E.A., L.A. Mackie, and C.E. Mullins. 1985. The use of plaster of Paris in the study of soil structure. Soil Use Manage. 1:70–72. doi:10.1111/j.1475-2743.1985.tb00660.x

Germann, P.F. and M. Karlen. 2016. Viscous-flow approach to in situ infiltration and in vitro saturated hydraulic conductivity determination. Vadose Zone J. 15(2). doi:10.2136/vzj2015.05.0065.

Greve, A.K., M.S. Andersen, and R.I. Acworth. 2010. Investigations of soil cracking and preferential flow in a weighing lysimeter filled with cracking clay soil. J. Hydrol. 393:105–113. doi:10.1016/j.jhydrol.2010.03.007

Hudak, P., B. Sadler, and B. Hunter. 1998. Analyzing underground water-pipe breaks in residual soils. Water Eng. Manage. 145:15–20.

Hunt, A.G. 2001. Applications of percolation theory to porous media with distributed local conductances. Adv. Water Resour. 24:279–307. doi:10.1016/S0309-1708(00)00058-0

Jabro, J.D., and W.M. Iversen. 2015. Nondestructive analysis of three-dimensional objects using a fluid displacement method. Soil Sci. Soc. Am. J. 79:1289–1292. doi:10.2136/sssaj2015.06.0215

Jones, L.D., and I. Jefferson. 2012. Expansive soils. In: J. Burland, editor, ICE manual of geotechnical engineering. ICE Publ., London. p. 1–46.

Kishné, A.S., C.L.S. Morgan, and W.L. Miller. 2009. Vertisol crack extent associated with gilgai and soil moisture in the Texas Gulf Coast prairie. Soil Sci. Soc. Am. J. 73:1221–1230. doi:10.2136/sssaj2008.0081

Krohn, J.P., and J.E. Slosson. 1980. Assessment of expansive soils in the United States. In: D. Snethern, editor, Proceedings of the 4th International Conference on Expansive Soils, Denver, CO. 16–18 June 1980. Vol. 1. Am. Soc. Civ. Eng., New York. p. 596–608.

Lin, H.S., K.J. Mclnnes, L.P. Wilding, and C.T. Hallmark. 1998. Macroporosity and initial moisture effects on infiltration rates in Vertisols and vertic intergrades. Soil Sci. 163:2–8. doi:10.1097/00010694-199801000-00002

Miller, W.L., A.S. Kishné, and C.L. Morgan. 2010. Vertisol morphology, classification, and seasonal cracking patterns in the Texas Gulf Coast prairie. Soil Surv. Horiz. 51:10–16. doi:10.2136/sh2010.1.0010

Návar, J., J. Mendez, R.B. Bryan, and N.J. Kuhn. 2002. The contribution of shrinkage cracks to bypass flow during simulated and natural rainfall experiments in northeastern Mexico. Can. J. Soil Sci. 82:65–74. doi:10.4141/S00-047

Neely, H.L. 2014. Spatial and temporal distribution of desiccation cracks in shrink–swell soils. Ph.D. diss. Texas A&M Univ., College Station.

Neely, H.L., J.P. Ackerson, C.L.S. Morgan, and K.J. McInnes. 2014. Instrumentation to measure soil subsidence and water content in a single borehole. Soil Sci. Soc. Am. J. 78:1251–1257. doi:10.2136/sssaj2014.02.0055n

Newman, E.I. 1966. A method of estimating the total length of root in a sample. J. Appl. Ecol. 3:139–145. doi:10.2307/2401670

Ringrose-Voase, A.J., and W.B. Sanidad. 1996. A method for measuring the development of surface cracks in soils: Application to crack development after lowland rice. Geoderma 71:245–261. doi:10.1016/0016-7061(96)00008-0

Sanders, E.C., M.R. Abou Najm, R.H. Mohtar, E. Kladivko, and D. Schulze. 2012. Field method for separating the contribution of surface-connected preferential flow pathways from flow through the soil matrix. Water Resour. Res. 48:W04534. doi:10.1029/2011WR011103

Shipitalo, M.J., V. Nuutinen, and K.R. Butt. 2004. Interaction of earthworm burrows and cracks in a clayey, subsurface-drained, soil. Appl. Soil Ecol. 26:209–217. doi:10.1016/j.apsoil.2004.01.004

Stavridakis, E.I. 2006. Assessment of anisotropic behavior of swelling soils on ground and construction work. In: A.A. Al-Rawas and Z.F.A. Goosen, editors, Expansive soils: Recent advances in characterization and treatment. Balkema, Leiden, the Netherlands. p. 371–384. doi:10.1201/9780203968079.pt7

Stewart, R.D., M.R. Abou Najm, D.E. Rupp, J.W. Lane, H.C. Uribe, J.L. Arumí, and J.S. Selker. 2015. Hillslope runoff thresholds with shrink–swell clay soils. Hydrol. Processes 29:557–571. doi:10.1002/hyp.10165

Stewart, R.D., M.R. Abou Najm, D.E. Rupp, and J.S. Selker. 2012. Measurement tool for dynamics of soil cracks. Vadose Zone J. 11(2). doi:10.2136/vzj2011.0048

Stewart, R.D., M.R. Abou Najm, D.E. Rupp, and J.S. Selker. 2014. Nondestructive quantification of macropore volume using shear-thinning fluid. Soil Sci. Soc. Am. J. 78:445–453. doi:10.2136/sssaj2013.08.0346

te Brake, B., M.J. van der Ploeg, and G.H. de Rooij. 2013. Water storage change estimation from in situ shrinkage measurements of clay soils. Hydrol. Earth Syst. Sci. 17:1933–1949. doi:10.5194/hess-17-1933-2013

Watson, K.W., and R.J. Luxmoore. 1986. Estimating macroporosity in a forest watershed by use of a tension infiltrometer. Soil Sci. Soc. Am. J. 50:578–582. doi:10.2136/sssaj1986.03615995005000030007x

Weisbrod, N., M.I. Dragila, U. Nachshon, and M. Pillersdorf. 2009. Falling through the cracks: The role of fractures in Earth–atmosphere gas exchange. Geophys. Res. Lett. 36:L02401. doi:10.1029/2008GL036096

Wopereis, M.C.S., J. Bouma, M.J. Kropff, and W. Sanidad. 1994. Reducing bypass flow through a dry, cracked and previously puddled rice soil. Soil Tillage Res. 29:1–11. doi:10.1016/0167-1987(94)90097-3

Zein El Abedine, A., and G.H. Robinson. 1971. A study on cracking in some Vertisols of the Sudan. Geoderma 5:229–241. doi:10.1016/0016-7061(71)90012-7

Zhang, Z.B., H. Zhou, Q.G. Zhao, H. Lin, and X. Peng. 2014. Characteristics of cracks in two paddy soils and their impacts on preferential flow. Geoderma 228–229:114–121. doi:10.1016/j.geoderma.2013.07.026